



Article

Optimization of Surface Cleaning and Painting Methods for DIC Measurements on Automotive and Railway Aluminum Materials

Szabolcs Szalai ¹, Viktória Fehér ¹, Dmytro Kurhan ² , Attila Németh ^{1,*} , Mykola Sysyn ³ and Szabolcs Fischer ^{1,*}

¹ Central Campus Győr, Széchenyi István University, H-9026 Győr, Hungary

² Department of Transport Infrastructure, Ukrainian State University of Science and Technologies, UA-49005 Dnipro, Ukraine

³ Department of Planning and Design of Railway Infrastructure, Technical University Dresden, D-01069 Dresden, Germany

* Correspondence: nemeth.attila@sze.hu (A.N.); fischersz@sze.hu (S.F.); Tel.: +36-(96)-613-544 (S.F.)

Abstract: The preparatory operations of DIC (Digital Image Correlation) tests were investigated in this study, with special emphasis on specimen cleaning and painting operations. As it is well known, DIC tests are non-contact and applied in materials research, the analysis of complex structures, and, nowadays, the construction industry. The use of DIC technologies has seen a dynamic increase in all scientific fields. In our study, aluminum body panels for automotive and railway applications were tested using this technique. There are many articles on proper patterning in the literature but fewer on preparation and priming. These are critical for a successful DIC measurement. This paper looks at different surface cleaners and primers with different grading procedures and will also determine the time window within which the paint should be applied. Finally, the GOM ARAMIS system was applied to measure and characterize the painted surface and visible deformation defects resulting from inadequate painting.

Keywords: speckle pattern; DIC; painting; surface cleaning; GOM ARAMIS; automotive aluminum



Citation: Szalai, S.; Fehér, V.; Kurhan, D.; Németh, A.; Sysyn, M.; Fischer, S. Optimization of Surface Cleaning and Painting Methods for DIC Measurements on Automotive and Railway Aluminum Materials.

Infrastructures **2023**, *8*, 27.

<https://doi.org/10.3390/infrastructures8020027>

Academic Editors: Ján Dižo, Rafał Melnik, Stasys Steišūnas and Miroslav Blatnický

Received: 19 January 2023

Revised: 1 February 2023

Accepted: 3 February 2023

Published: 6 February 2023



Copyright: © 2023 by the authors. Licensee MDPI, Basel, Switzerland. This article is an open access article distributed under the terms and conditions of the Creative Commons Attribution (CC BY) license (<https://creativecommons.org/licenses/by/4.0/>).

1. Introduction

Numerous techniques for measuring strain and displacement are described in international books and papers. Conventional measurement methodologies comprise, among others, of extensometers and linear variable differential transformers. These measurement technologies need much preparatory work and costly equipment and apparatus.

3D-DIC is a technique that can detect the 3-dimensional position, total displacement, and stretch field of an object without touching it. It is a very effective and flexible tool for measuring the shape, movement, and deformation of different materials and structures. Using CCD (charged-coupled device) cameras and a constant white light source, it takes images of the object at predetermined intervals, first while the undeformed piece is still in the reference state and then continuously while it is deforming. The cameras can measure the deformation accurately and precisely if the three main components are present. The first element is for applying the appropriate pattern, then taking the necessary images, and finally analyzing the saved images using analytical software [1,2].

Digital Image Correlation can be applied in research, projects, and studies related to the following fields: (i) engineering, (ii) material science, (iii) physics and astronomy, (iv) computer sciences, (v) Earth and planetary sciences, (vi) chemical engineering, (vii) chemistry, (viii) environmental science, (ix) agricultural and biological sciences, (x) energy, (xi) biochemistry, genetics and molecular biology, (xii) medicine, (xiii) arts and humanities, (xiv) dentistry, (xv) neuroscience, etc. Since this paper explores engineering and material

science, the authors would like to describe some examples from these fields in the following paragraphs. In addition, it should be noted that the introduced literature covers only a small part of the possibility of the application of the DIC technique, as more than 80,000 papers have been published on the topic of DIC since 1990 on the Google Scholar database (these data are approx. 17,000 in Scopus and about 12,500 in Web of Science). It is worth mentioning that compared to these values, the traditional ESPI technology (i.e., electronic speckle pattern interferometry) has 10,000, 1700, and 900, respectively).

Referring to the above paragraph, approximately 160 and 12 articles have been published in 2022 and 2023, respectively, indexed in the Scopus database, with titles that contain the word DIC. Furthermore, there are approximately a thousand documents between 2001 and 2023. Engineering, material sciences, physics, and astronomy are the most significant areas. The top-cited papers are the following [3–7]. Among the new articles, [8–12] documents are worth mentioning. According to the above trends, DIC techniques are and will be significant parts of research and development in the future.

The most relevant literature is described and summarized in the following paragraphs and Sections 1.1 and 1.2.

Ye et al. [13] configured a reflection-assisted multi-view DIC system that contains a stereo-DIC (SDIC) unit and a reflection-assisted stereo-DIC (RSDIC) unit. They aimed to apply simultaneous measurement for external and internal surface shape and deformation using the DIC technique, focusing on cavity structure. Their laboratory tests proved that the accuracy of shape and thickness measurements could be within 0.03 mm, while the deformation measurement accuracy is within 62 microns. Ye et al. showed that their method is adequate and helpful for the aero-engine casing.

Pupurs et al. [14] applied DIC measurement methodology for stiffness determination of damaged laminates. The main goal was the solution of the related validation as well as the introduction and representation of the connecting engineering approach. Their study dealt with composite cross-ply laminates with evolving micro-damage during 4-point bending tests. The considered structures were carbon/epoxy and glass/epoxy cross-laminated plywood. They aimed to determine the midplane curvature of these structures. There were composed finite element (FE) models for validating DIC measurements. They concluded that the combination of applied beam theory and the DIC deformation measurement solution was appropriate enough; however, the considered beam theory underestimated a little bit the real deformations.

Suthar et al. [15] carried out research regarding the post-necking behavior of aluminum alloys and special friction stir weldings (FSW) using these materials. They performed laboratory experiments and considered rectangular tensile specimens during uniaxial tensile tests. The DIC technique supplemented the measurements with two cameras that monitored the deformation of the specimens. The applied method is similar to GOM ARAMIS, also utilized in the current study. For validation, the so-called Hill's normal anisotropic yield criterion was considered; it helped determine post-necking behavior. In addition, the shown experimental method successfully forecasts the area in the FSW joint at the necking section, where the existing inhomogeneity is challenging to capture using an analytical approximation.

Bhuiyan et al. [16] presented solutions for using DIC in learning traditional mechanics. This paper demonstrates how a simple, quickly transportable experimental setup, the SB-DIC (stress-block coupled DIC), demonstrates how deformation fields on a surface change under different external loads and how this experiment helps students improve their learning process. It can also be used in a real but interactive classroom, too. The authors investigated how this procedure and methodology help students better understand classical mechanics at school and at home. After conducting a qualitative and quantitative data analysis, Bhuiyan et al. found that SB-DIC enhances students' previous knowledge.

Zhou et al. [17] examined sandstone using DIC. The authors' goal was to determine red sandstone's failure and mechanical behaviors if it has a flaw (mainly pre-existing) during compressive-shear loading. The specimens were square-shaped, and the dimensions were

100 × 100 × 30 mm (width × height × thickness, respectively). The single flaw inside them was approximately 20–40 mm long and 1–3 mm wide, mainly located diagonally, but there were also at 15, 30, and 60-degree directions. Zhou et al. analyzed the die angle on failure behaviors considering the pre-flaw characteristics. The results can be formed based on the laboratory tests supplemented by DIC measurements. The authors took into consideration the novel crack's dominant parameter during the evaluation process of the results.

Wang et al. [11] investigated thin films and their out-of-plane displacements with the application of the DIC method. The considered DIC technique was a special mechanical constrained-based 3D-DIC. To be able to determine the films' displacement, a mesh of 8-node rectangular hemispheres (i.e., shell elements) was used. The main principle was to ensure spatial continuity. In addition, a blistering test was carried out, and the results demonstrate that the 3DMC-DIC (three-dimensional subset-based digital image correlation) method can achieve a spatially continuous and highly accurate thin film planar displacement field at the sample edge.

Li et al. [18] dealt with the mechanical behavior of anchored rock with an infilled joint under uniaxial loading. The applied methods were acoustic emission and DIC. The connecting tests were laboratory experiments, The considered rock was sandstone, and the filling material was cement. The cement slurry specimens were cured for seven days considering constant humidity and temperature. First, Brazilian tests were conducted to determine the materials' mechanical characteristics, i.e., tensile strength values. After that, additional specimens were tested with bolts (type 304 stainless steel, diameter of 3.5 mm, an elastic modulus of 198 GPa, a Poisson's ratio of 0.3, and a tensile yield strength of 450 MPa). Epoxy resin was applied as the bonding material between the bolt and rock. This bolt simulated the so-called anchor during the laboratory experiments, i.e., the direct shear tests. Specimens were categorized into three groups: crack evolution of specimens with an angle of 30°, 60°, and 90°. All of the measurements were evaluated using the video recording of DIC measurements.

Among the above-introduced examples, the DIC optical measurement technology and assessment method can be applied in the future, e.g., in engineering structures [2,19,20], railroads [21–25], road construction [26–29], aircraft [30,31], “navitics” (or in other words, navigation) [32], astronautics [33,34], and so on.

In this research, the authors applied an approach regarding railway and automotive vehicles and their car body sheets.

1.1. Overview of DIC Technology

The DIC technique, therefore, offers the possibility of mechanical, qualitative, and quantitative testing of materials under load conditions. The images taken by the CCD camera are counted as a single load step. The standard cameras use a photosensitive cell with 1024 × 1280 pixels or more. Each pixel stores one of the grayscale values corresponding to the intensity of the reflected light. The method runs a 2 × 2 window through the binary image, with the frames weighted by powers of 2, representing 1, 2, 4, and 8 values, respectively. It identifies a patch with a well-defined unique feature and then runs it through the entire sequence of deformation images to obtain the local deformation of the patches. These deformations are then fitted to the mesh, which can register the deformation properties of each element.

The DIC technique has long been known as “speckle correlation”. However, this name is not “random”, as the system can only perform the necessary measurements if it has a good view of the object, which is made possible by the pattern applied to the surface. To be able to obtain a good pattern, it is essential to take into account four factors: the size of the speckles, contrast, spatial distribution, and sharpness of the edges of the speckles [35].

The size of the spots is one of the critical points, as the aim is usually to keep them as small as possible, but they may eventually become so small that the system can no longer detect them. Research shows that the optimum size is at least three pixels, but this value does not tell someone how many millimeters it should be physically. If the spots are smaller

than three pixels, they cannot be detected. Therefore, not only the size of the patches is essential, but also the size of the subset. It is also a critical point in measurements, as a subset must contain at least three spots [36,37].

Regarding the density of spots, it is ideal to have the same size of the white and black area. With printing, this is very easy to do, as everything can be adjusted manually. However, with spray paint, it is not so easy; it is easy to overdo it, as the mist can quickly spread over the object, resulting in poor contrast [36].

The patches' spatial distribution is vital in the horizontal and vertical directions and plays a decisive role in the analysis from all orientation directions. Having patches in all directions is essential, which is why random sampling is preferable. Care should be taken to ensure that, where possible, the orientation is also random [38].

Overall, based on the above, it is imperative that the pattern on the surface has high contrast, that the greyscale intensity varies, and that it is random, not periodic, and not repetitive. A spot should be somewhere between three and five pixels. A good pattern should adhere tightly to the surface and deform with the surface of the specimen [1].

Different methods of speckle patterning are known in the literature. One of the best-known methods is spraying white or black paint using a gas-powered bottle or airbrush. With this method, many variables must be considered, such as the nozzle diameter, the substrate, the distance between the nozzle and the piece, the pressure, and even the viscosity of the solution. These factors all affect the spots' size, distribution, and dispersion. In most cases, commercially available white or black spray paints are applied, whose application is recommended at room temperature by the manufacturer [39,40].

1.2. Formability Tests Using DIC Measurement

There are various tests for the formability of metal sheets. One of the simplest and most frequently used is Erichsen's tensile test [41], along with the more complex Nakajima and Marciniak tests [42,43]. The Erichsen test can be used to test formability and extensibility under constant load. The Nakajima and Marciniak tests are usually applied to obtain a forming limit diagram (FLC) using a 100 mm hemispherical forming punch using specimens with different geometries. One of the most well-known plate formability methods is the Erichsen test. The test can be performed for plates thinner than 3 mm. The measurement lasts until the crack appears on the surface of the test piece. The displacement of the punch measured at the time of cracking will give the result of the Erichsen test, the *IE* number [44,45].

The total displacement and strain field of sheet metal specimens subjected to the Erichsen test can be determined using multi-camera DIC equipment. These DIC devices track the deformation of the specimen during the stretching-drawing process. The only problem with 2D-DIC systems is that the camera must be well-aligned for accurate measurement; otherwise, it cannot handle out-of-focus deformations during the forming process. The improved stereo DIC tracks 3D deformation; the camera positioning is flexible [46].

In the research on this topic, it was suggested that multi-camera DIC tools employ a so-called master camera that should be selected from all the cameras, which takes the initial captured camera image as a reference, and the other images are all corrected and compared with this reference image [47].

Erichsen tests have been performed to determine the resistance of coatings to failure [48]. The process and forming involve using a hemispherical punch to test the fracture (destruction) of the coating layer. Similar tests in industrial applications are primarily evaluated for quality control purposes. The result is a yes/no rating based on whether the coating meets the deformation specifications. Color coatings are mainly applied for external aesthetic purposes, possibly for protection. When evaluating coatings, it is essential to note that resistance to crack is a fundamental requirement, but it should be remembered that good adhesion to the substrate is also of paramount importance. The authors of the mentioned article use a finite element model (FEM) to demonstrate the surface deformations during the implementation of the Erichsen test. The article compares

the predicted deformations and the deformations experimentally determined by DIC. The deformation characteristics were evaluated for each result, and the expected location of the coating failure was subsequently predicted. The experiment was performed using GOM ARAMIS, and the results were analyzed using GOM Correlate Professional software. In the experiment conducted by Sorce et al. [48], the steel plate failed before coating in all of the Erichsen cupping tests, indicating that the ductility of the coating was more adequate than the steels [48].

It is clear from the literature reviewed that the quality and accuracy of the DIC test result depend on the quality of the painted speckle pattern and the optimum paint adhesion to the test specimen. This research focuses on testing primer paints for DIC testing on aluminum sheet materials. The surface preparation techniques are also crucial in the paint qualification since proper paint adhesion can only be achieved on a well-prepared surface. Ease of application and accessibility were the main criteria for selecting paints and preparation (cleaning) materials. The aim of the tests is to determine the methods to prepare aluminum sheets used in the automotive industry and the production of railway carriages or motor train bodies for DIC tests. The results will allow someone to safely carry out DIC test preparation operations for laboratory tests and DIC measurements under real conditions of use. The research is also relevant because there is very little literature on the control of paint adhesion, which is of paramount importance since the results of DIC testing can only be as good as the ability to achieve a properly adhesive basecoat.

1.3. The Novelty of the Current Study and the Structure of the Paper

Based on the literature review shown in Sections 1.1 and 1.2, the authors have decided to investigate the suitability and applicability of a combination of commercially available cleaning agents and paint sprays on five different types of aluminum plates for DIC-based optical deformation measurements combined with Erichsen cupping tests. The authors applied DIC measurements. The instrument was a GOM ARAMIS 5M system. The qualification of the paintings started with a series of measurements according to international standards. These were the so-called pre-filters for the Erichsen cupping test.

The structure of the paper is the following: in Section 2, the applied materials and methods are detailed. Section 3 describes the results, and Section 4 contains the derived conclusions.

The laboratory experiments were performed by wet paint film thickness tests (Section 3.1), touch tests (Section 3.2), print-free tests (Section 3.3), cross-cut tests (Section 3.4), bending tests (Section 3.5), Erichsen tests with DIC evaluation and traditional dial gauge measurement (Sections 3.6 and 3.7), as well as durability tests (Section 3.8).

2. Materials and Methods

The research focused on investigating commercially available surface preparation, cleaning materials (cleaning agents), and spray paints used in industrial and laboratory research processes. The manufacturer's recommendations were also considered in the surface preparation materials' selection procedure. During the selection of paints, in addition to easy accessibility, spray formulation/packaging and ease of use, preferably certification for indoor use rating, were essential criteria. Twelve pieces of surface cleaner, eleven pieces of paint, and five pieces of aluminum sheet material (material plate) were tested during the tests.

Due to the fact that the authors have more than 10 years' experience in DIC measurements, we could guarantee the preparation of adequate, appropriate, and identical painting would result in the same speckle pattern for all the specimens.

2.1. Materials

Table 1 contains the used surface preparation and cleaning detergents and liquids.

Table 1. The used surface preparation materials.

ID	Name	Brand
SC1	Brigéciol D-3	Kemobil
SC2	9973 engine washer	Mannol
SC3	Diluent/diluter 513	Egokorr Izofix
SC4	H-100 synthetic diluent	Supralux
SC5	Acetone UN1090	Styro-Flow
SC6	Nitro diluent UN1263	Styro-Flow
SC7	Contact cleaner	Chip Medikémia
SC8	Brake cleaner	Engelnert Strauss
SC9	Cold degreaser	Welldone
SC10	Isopropyl alcohol	Gyórlakk
SC11	Detergent water	Ludwik
SC12	Dry cleaning with wipes	Tork 652100

The goal was to test white color paints with good coverage characteristics in spray form easily available commercially. Furthermore, the measurements often must be performed in non-laboratory conditions or in an inadequately equipped laboratory, where the airbrush system is impossible to use. Another aspect of the selection is that the paint should be suitable for indoor use and application with personal respiratory protection equipment. Finally, the reason for choosing the white color is that the random pattern of spots must be applied to avoid accidental painting with black paint, and the best contrast is achieved with a white base color primer. Table 2 summarizes the selected paints.

Table 2. List of the applied paints.

ID	Name	Manufacturer	Gloss (Matte or Silk)	Color (RAL Color Code)	Base (min 40%)
P1	Acrylic Primer	Maestro	Matte	RAL9003	Acetone + Xylol
P2	Acrylic Mat Primer	Maestro	Matte	RAL9003	Acetone
P3	High Temp. Paint	Maestro	Silk	RAL9003	Acetone + Xylol
P4	Heat Resistant	Motip	Matte	04036 (white)	Silicone Resin
P5	Spray Putty	Motip	Matte	04062 (beige)	Acrylic resin
P6	Acrylic	Prisma Color	Silk	RAL9010	Aceton + Ethyl acetate
P7	Acrylic	Prisma Color	Silk	RAL9016	Aceton + Ethyl acetate
P8	Radiator	Prisma Color	Silk	91152 (white)	Aceton + Ethyl acetate
P9	Aqua Eco+	Dupli-Color	Matte	RAL9010	Water + Acetone
P10	Chalk Finish Broken white	Pinty Plus	Matte	CK788	Water + Acetone
P11	HB Body 950	HB Body	Matte	White	Caoutchouc + Syntetic Resin

Aluminum sheets used in the automotive industry and the production of railway vehicle bodies were selected for the research. Body materials with sub-optimal composition and surface coating must be applied in industrial practice. Regarding sheet thicknesses, the most common sizes have also been selected, depending on the stocks of raw materials and availability. Table 3 shows the five materials selected according to these criteria.

Table 3. Aluminum sheet materials used for painting tests.

ID	Material Quality	Thickness [mm]
A11	AlMgSi3	1.5
A12	AlMgSi3	2.5
A13	TL091	1.0
A14	TL094	0.65
A15	Al99	0.22

2.2. Measurement Methods and Instruments

The measurement procedure and the instruments are the same as in the authors’ previous paper [49]. Therefore, to be able to avoid the high similarity rate, this section has been omitted.

As a short overview, the executed tests were the following:

- Wet paint film thickness measurement by Elcometer 112Al wet film comb, according to [50].
- Touch test, which is a subjective measurement procedure.
- Print-free test according to [51,52]. During the test, a 26 mm diameter circular paper (80 g/m²) is placed on the painted surface, followed by a 22 mm diameter 5 mm thick rubber element (hardness 50 IRHD ± 3 IRHD). The utilized weights on this rubber element were: 20 g, 200 g, 500 g, and 1000 g.
- Cross-cut test by Elcometer 107 cross-hatch cutter in accordance with [53].
- Bending test based on [54,55]. The instrument’s cylinder’s diameter was 20 mm, the specimens’ dimension was square: 90 × 90 mm,
- Erichsen cupping test according to [56] with the supplementary evaluation of GOM ARAMIS 5M DIC system.
- Plate thickness test executed by a Mitutoyo dial gauge.

The details of these tests are described in [49].

3. Results and Discussion

For each test (see Section 2.2), the painting/cleaning techniques are highlighted where they have scored positively or negatively.

3.1. Wet Paint Film Thickness Measurement

Table 4 summarizes the related measurements’ results, demonstrating that all paints coat the base plate in almost the same layer. It should be mentioned that only one paint (P11) resulted in relevant variations. The paint layer can crack during drying in the case the paint’s thickness is too big, which means danger. When the results (Table 4) are evaluated and analyzed, it can be concluded that there are no significant and considerable differences between the different cleaning methods and raw materials used.

Table 4. Results of the wet paint thickness measurement.

ID.	Name	Paint Thickness [µm]		
		Lower Limit	Upper Limit	Average
P1	Acrylic Primer	100	125	112.5
P2	Acrylic Mat Primer	100	125	112.5
P3	High Temp. Paint	75	100	87.5
P4	Heat Resistant	125	150	137.5
P5	Spray Putty	125	150	137.5
P6	Acryl	125	150	137.5
P7	Acryl	125	150	137.5
P8	Radiator	50	75	62.5

Table 4. *Cont.*

ID.	Name	Paint Thickness [μm]		
		Lower Limit	Upper Limit	Average
P9	Aqua Eco+	75	100	87.5
P10	Chalk Finish Broken white	125	150	137.5
P11	HB Body 950	600	650	625

3.2. Touch Test

Since the dyes resulted in a bubbly, blotchy surface on some materials, it was necessary to exclude two cleaning agents (SC6, SC10). These cleaning procedures were not used in further tests because using such dyes is inappropriate and not allowed for the DIC measurement procedure. Table 5 presents the results of the touch test.

Table 5. Results of the touch test.

ID.	Name	Drying Time [min]
P1	Acrylic Primer	35
P2	Acrylic Mat Primer	35
P3	High Temp. Paint	35
P4	Heat Resistant	35
P5	Spray Putty	15
P6	Acryl	15
P7	Acryl	15
P8	Radiator	20
P9	Aqua Eco+	45
P10	Chalk Finish Broken white	5
P11	HB Body 950	25

The surface defects are shown in Figure 1. SC6 left bubbles and SC10 left spots on the test surfaces. The results summarized in Table 5 show that there were no significant differences between the different cleaning methods and the raw materials used. Therefore, these results are not shown in Table 5.

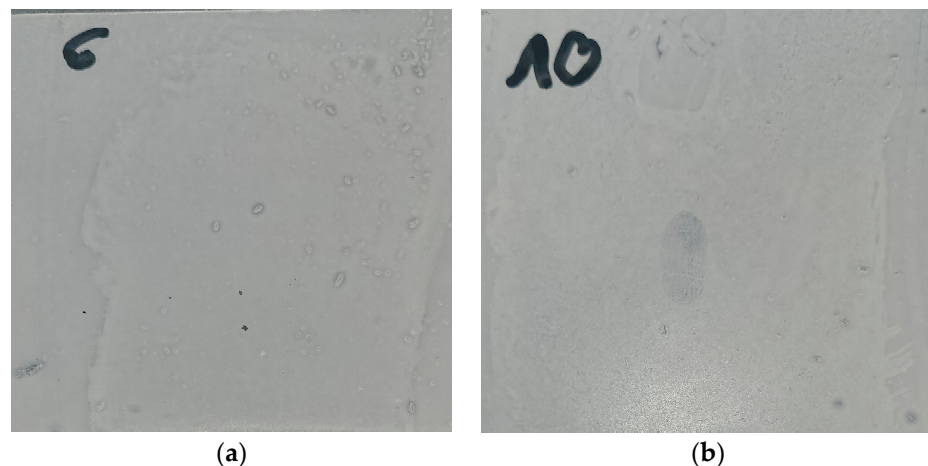


Figure 1. Photos of consequences of inadequate procedures. (a) SC6 left bubbles on the test surface; (b) SC10 left spots on the test surface.

3.3. Print-Free Test

The timing of the touch tests marked the start of the print-free tests. After this time, the measurement windows followed each other every 15 min. Drying times up to 1000 g are shown in Table 6.

Table 6. Print-free drying time.

ID.	Name	Print-Free Drying Time [min]
P1	Acrylic Primer	50
P2	Acrylic Mat Primer	35
P3	High Temp. Paint	35
P4	Heat Resistant	35
P5	Spray Putty	45
P6	Acryl	30
P7	Acryl	45
P8	Radiator	35
P9	Aqua Eco+	165
P10	Chalk Finish Broken white	20
P11	HB Body 950	70

The results were assessed without excluding either paints or other cleaning processes. No differences could be detected between the different cleaning methods and raw materials used; therefore, these data are not included in Table 6.

3.4. Cross-Cut Test

Table 7 shows the results of the cross-cut test. From the results, many deductions can be derived. All the A11–A15 samples behaved similarly as there was no difference in the measurement results for the different raw materials. From this, it can be drawn that neither the substrate nor the plate thickness has any relevant role in the paint adhesion, only the surface quality. Different results than expected were also obtained concerning test times. Even after 0 (immediate measurement after print-free drying time), 6, 12, or 24 h, there were no difference in results. The “OK” samples tested well both at the beginning and at the end of the measurements. The “NOK” samples did not perform well in some measurement phases and were disqualified from further testing. Stains P1, P2, P6, P7, P10, and P11 failed and had to be disqualified from further testing. Cleaners SC3, SC7, and SC11 were disqualified because they did not ensure good adhesion to the plate, even for paints that achieved good ratings.

Table 7. Results of the cross-cut test.

ID.	Name	Materials: A11–A15									
		Drying Time: 0, 6, 12, 24 h									
		SC0	SC1	SC2	SC3	SC4	SC5	SC7	SC8	SC9	SC11
P1	Acrylic Primer						NOK				
P2	Acrylic Mat Primer						NOK				
P3	High Temp. Paint			OK				NOK	NOK	OK	NOK
P4	Heat Resistant						OK				
P5	Spray Putty	OK	NOK	OK	NOK	NOK	NOK	NOK		OK	
P6	Acryl						NOK				
P7	Acryl						NOK				
P8	Radiator		OK		NOK		OK	NOK	OK		NOK
P9	Aqua Eco+	OK		NOK			OK	NOK		OK	
P10	Chalk Finish Broken white						NOK				
P11	HB Body 950						NOK				

Based on the analysis of the measurement results obtained, it can also be concluded that proper adhesion can be achieved within 24 h after the print-free test, independently of the quality of the plate, utilizing a reasonable staining/cleaning procedure. For this reason, in order to verify formability, the following sequential tests were performed only and exclusively for the remaining combinations.

3.5. Bending Test

According to the bending test results, the first conclusion was that P5 and P8 paints were poorly milky when all the other residual cleaning agents were used in the tests (see Table 8). The bending test, combined with the cross-cut test, provided the result that the paint did not follow the deformation of the plate along the cut of the paint because it was separated from the plate. This phenomenon and result are illustrated by the photos of the tested samples under the microscope in Figure 2.

Table 8. Results of the bending test.

ID.	Name	Materials: A11-A15						
		Drying Time: 0, 6, 12, 24 h						
		SC0	SC1	SC2	SC4	SC5	SC8	SC9
P3	High Temp. Paint				OK			
P4	Heat Resistant				OK			
P5	Spray Putty				NOK			
P8	Radiator				NOK			
P9	Aqua Eco+				OK			

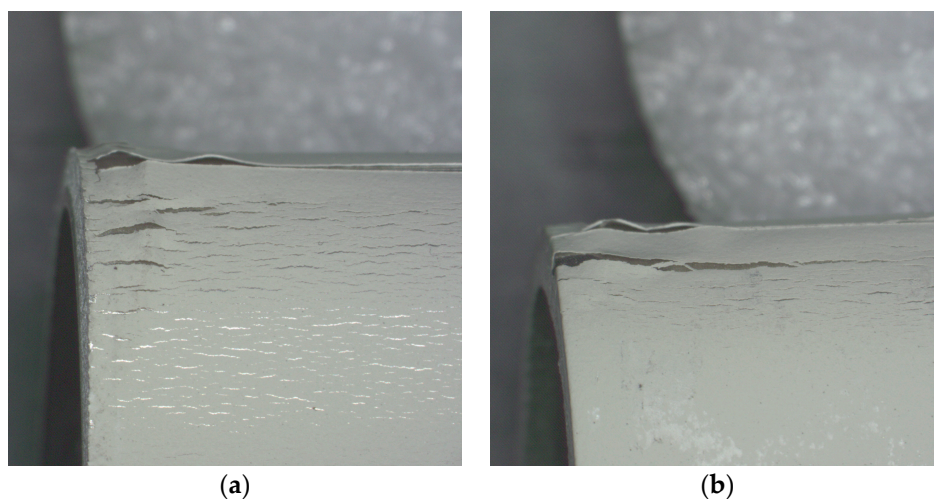


Figure 2. Microscopic images of paints. (a) P5's and (b) P8's.

The photos (see Figure 2) show the paint peeling off, while Figure 3 shows the corresponding paint layers. It can be seen that good contact (adhesion) was achieved between the paint and the base aluminum plate (see Figure 3).

3.6. Erichsen Test Results by Visual Inspection

The Erichsen test was first used to detect the appearance of staining. It was determined that the measurements accurately simulated the deformations expected during plate tests or plate forming processes, and thus appropriate deductions could be drawn about the paint-plate relationships. Table 9 shows the results and clearly shows that the remaining three paints tested well with all seven cleaning agents (SC0, SC1, SC2, SC4, SC5, SC8, SC9).

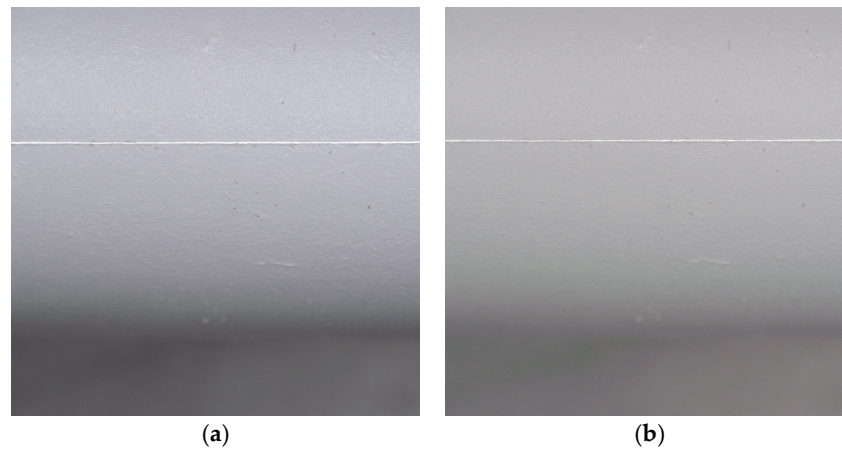


Figure 3. Results of a successful bending test. (a) adequate result achieved by P3 paint; (b) adequate result achieved by P9 paint.

Table 9. Results of the visual inspection of the Erichsen test.

ID.	Name	Materials: Al1–Al5						
		Drying Time: 0, 6, 12, 24 h						
		SC0	SC1	SC2	SC4	SC5	SC8	SC9
P3	High Temp. Paint				OK			
P4	Heat Resistant				OK			
P9	Aqua Eco+				OK			

3.7. Results of DIC Tests, Comparison of Thickness Reductions

The Erichsen tests were carried out with the DIC measurement technique considering the remaining staining/cleaning procedures. In the first round of measurements, the paints were visually qualified; see Section 2 in [49]. Thickness reduction (−eps3) values were determined for each specimen during DIC measurements, which could be performed after the rating.

All specimen types achieved a satisfactory (1) rating within 24 h using three painting (P3, P4, and P9) and seven cleaning procedures (SC0, SC1, SC2, SC4, SC5, SC8, SC9)—taking into account the results of the visual inspection. No differences in ratings were observed, and the analysis continued with the DIC assessment.

Figures 4 and 5 show the GOM ARAMIS assessment pictures of the aluminum specimen plate and the thickness reduction results along the length section of the sample. For each painting and cleaning procedure, this evaluation method was performed on each specimen.

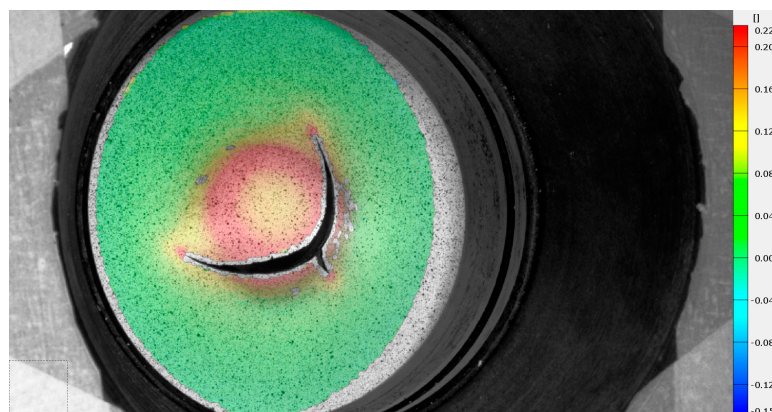


Figure 4. Al99 sample plate with P9/SC9 painting and cleaning process (dimensions are in mm).

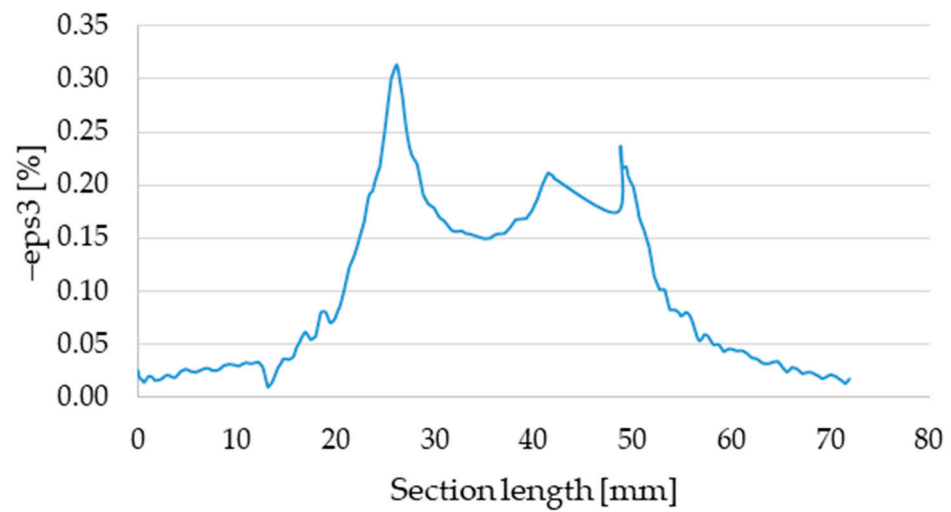


Figure 5. Thickness reduction values for the P9/SC9 sample.

To study the performance of the coatings (paintings) further, the thickness reduction values at the peak and their average were collected for each sample. Table 10 provides a summary of these results.

Table 10. Thickness reduction results measured at the apex of the test specimen using different painting/cleaning procedures.

ID	Name	Materials: A15						
		Thickness Reduction: AVG $-\text{eps3}$ [%]						
		SC0	SC1	SC2	SC4	SC5	SC8	SC9
P3	High Temp. Paint	0.155	0.463	0.136	0.446	0.234	0.080	0.206
P4	Heat Resistant	0.163	0.501	0.138	0.418	0.242	0.083	0.221
P9	Aqua Eco+	0.154	0.466	0.120	0.352	0.433	0.422	0.069

During the DIC measurements, the GOM ARAMIS system determines the engineering elongations; the software updates the $-\text{eps3}$ values when calculating the thickness reduction. Therefore, to compare the thickness, it is necessary to establish a connection between the parameters of the engineering and logarithmic elongations. This relationship is described in the following formulas (Equations (1)–(3)).

$$\text{engineering elongation} : \varepsilon = \frac{l_1 - l_0}{l_0} \tag{1}$$

$$\text{logarithm elongation} : \varphi = \ln \frac{l_1}{l_0} \tag{2}$$

$$\text{relationship} : \varphi = \ln(1 + \varepsilon) \tag{3}$$

where ε is the engineering elongation (%), l_1 is the elongated length of the specimen (mm), l_0 is the undeformed length of the specimen (mm), and φ is the logarithm elongation (%).

After the calculation of the plate thickness changes, the relationships in Equations (4) and (5) can be achieved, from which the accurate thickness value can be determined.

$$\varphi_s = \ln \frac{s_1}{s_0} \tag{4}$$

$$\text{expressed in} : s_1 = s_0 \cdot e^{\varphi_s} \tag{5}$$

where φ_s is the logarithm elongation in thickness direction (%), s_0 is the initial plate thickness (mm), s_1 is the thinned plate thickness (mm), and e is the Euler-number.

Table 11 compares the results obtained by using the relationship in Equation (5) with the calculated results. The values of thickness reduction at the peak taken from ARAMIS and the results of the hourly measurements are represented in Table 11. The painting/cleaning process can be assessed because since the results are close, the tested process is suitable for DIC technology.

Table 11. Comparison of ARAMIS and thickness measurement results.

ID.	Name	Measuring Device	Materials: Al5						
			Thickness Reduction: Measured and Calculated [mm]						
			SC0	SC1	SC2	SC4	SC5	SC8	SC9
P3	High Temp. Paint	ARAMIS	0.22	0.15	0.22	0.15	0.20	0.23	0.20
		Gauge	0.22	0.16	0.22	0.15	0.19	0.22	0.20
P4	Heat Resistant	ARAMIS	0.21	0.14	0.22	0.16	0.20	0.23	0.20
		Gauge	0.20	0.16	0.21	0.17	0.19	0.23	0.21
P9	Aqua Eco+	ARAMIS	0.22	0.15	0.22	0.17	0.15	0.16	0.23
		Gauge	0.20	0.15	0.22	0.18	0.17	0.17	0.23

It can be stated, based on the above results, that it is clear that the deviations are all within the measurement error of the dial gauge (0.02 mm), so the DIC measurements give good results, i.e., the primer painting methods convey the shape change well.

The research deduced that thicker Al2 plates with a surface quality corresponding to a polished surface quality (Ra 0.005-0.05, ISO 2768 [57]) performed worse in this test (see Table 12).

Table 12. Measurement results of usability tests.

ID.	Name	Measuring Device	Materials: Al2						
			Thickness Reduction: $-\epsilon_{ps3}$ [%]						
			SC0	SC1	SC2	SC4	SC5	SC8	SC9
P3	High Temp. Paint	ARAMIS	1.97	1.99	1.91	1.87	1.95	1.94	1.99
		Gauge	2.19	2.23	2.19	2.29	2.20	2.26	2.24
P4	Heat Resistant	ARAMIS	1.95	2.01	1.96	1.97	1.98	1.99	1.88
		Gauge	2.19	2.21	2.20	2.17	2.19	2.23	2.21
P9	Aqua Eco+	ARAMIS	1.91	1.92	1.92	1.94	1.98	1.99	2.01
		Gauge	2.19	2.18	2.17	2.18	2.21	2.19	2.20

The results in the table above show more significant differences of over 15%. However, the other samples, which typically have a matt and “rougher” surface, show similar variations to Table 10. Therefore, it can be concluded that for excellent, almost polished surface aluminum, DIC measurement results can show a variation of 10–15%, and, therefore, surface roughening may be justified during surface preparation if the research task allows.

3.8. Durability Tests

A longer-term usability test was conducted to complement the results of the DIC studies. The Al2 sheet material was selected for testing with P3, P4, and P9 paints because these paints have tested best in previous measurements. For the selection of the cleaning agents, the three most readily available types (SC1, SC4, SC9), which are also used in industry, were selected from the seven types remaining in the “tank”. The Erichsen tests were repeated after a 24-h, one week, and two weeks waiting period. The study aimed to define the time window during which specimens can still be utilized. The test can simulate an extended shutdown of a measurement laboratory, where it is crucial to know whether or not a limited number of samples can still be used for DIC measurements.

Table 13 shows the averaged thickness measurement results, including the dial gauge and the ARAMIS measurements. It can be clearly seen that after one week, the paints were still well-behaved (also on the other Al samples), but after two weeks, the P4 and P9 paints were already destroyed, regardless of the surface cleaning procedure. Although the P3 sample did not peel and the measurement went all the way through, cracking had already appeared. Table 14 shows the rating results calculated from the measurement results, where deviations below 10% are adequate, but those above this can no longer be used safely to analyze plate formability processes. The 10% threshold is based on previous pre-experiments, and a 10% deviation is, in fact, a 10% measurement error, which is a significant and unacceptable deviation.

Table 13. Measurement results of usability tests (material: Al2, surface preparations: SC1, SC4, and SC9).

ID.	Name	Drying Time: 1 Week					
		Thickness from Gauge (AVG)	Thickness from ARAMIS (AVG)	Thickness from Gauge (AVG)	Thickness from ARAMIS (AVG)	Thickness from Gauge (AVG)	Thickness from ARAMIS (AVG)
P3	High Temp. Paint	2.26	2.05	2.24	2.03	2.28	2.10
P4	Heat Resistant	2.33	1.95	2.26	1.91	2.35	1.90
P9	Aqua Eco+	2.16	1.98	2.20	1.99	2.24	2.05
Drying Time: 2 Weeks							
P3	High Temp. Paint	2.30	2.08	2.25	2.06	2.07	1.97
P4	Heat Resistant	separated	–	separated	–	separated	–
P9	Aqua Eco+	separated	–	separated	–	separated	–

Table 14. Certification results of usability tests (materials: Al1–Al5, surface preparations: SC1, SC4, and SC9).

ID.	Name	Drying Time: 1 Week
P3	High Temp. Paint	OK (thickness reduction difference under 10%)
P4	Heat Resistant	NOK (thickness reduction difference more than 15%)
P9	Aqua Eco+	OK (thickness reduction difference under 10%)
Drying Time: 2 Weeks		
P3	High Temp. Paint	OK (thickness reduction difference under 10%)
P4	Heat Resistant	NOK (the paint separated)
P9	Aqua Eco+	NOK (the paint separated)

Figure 6 shows the Al2 sample painted with P9 paint and prepared with SC4 cleaner. The pick-up and flaking of the dye are clearly visible, which makes the DIC measurement practically unreadable.

The results show that the P3 paint can be used for up to two weeks with the SC1, SC4, and SC9 surface cleaning agents, but the same is not true for the other paints.

The following conclusions can be drawn based on the studies and results presented. Seven out of twelve surface cleaning agents showed promising results on all five materials, but it can be concluded that their effect is not indifferent. SC6 and SC10 produced a painted surface with all stains and on all materials, which cannot be used for DIC tests because if the base color is not homogeneous, it will cause a measurement error when evaluating the speckle pattern. The results of the grid cut tests are significant as they will show whether the paint/cleaner combinations can provide the correct adhesion to the surface of the plate samples.

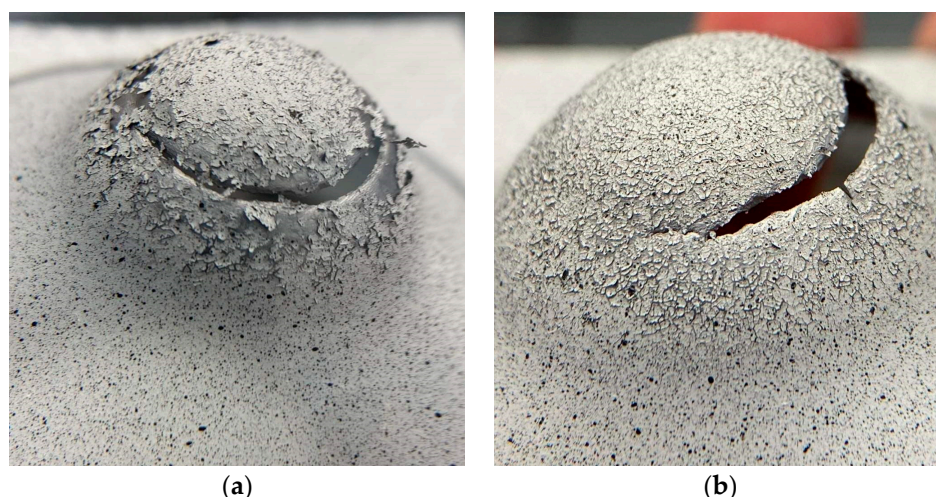


Figure 6. Separated paint after forming as shown for P9/SC4. (a) pick-up of the painting; (b) flaking of the painting.

The P1, P2, P6, P7, P10, and P11 paints did not produce satisfactory results with any of the cleaners within 24 h. Also, SC3, SC7, and SC11 were excluded here. These detergents failed to produce good adhesion with any paints and bases. The results at this point support the hypothesis that it is not indifferent as to which paint is used on aluminum materials and that attention should be paid to the choice of surface cleaning method.

The bending test combined with scratching also gave essential results. The procedure can well characterize hidden paint peeling. In the pre-tests, it was repeatedly found that the bent test specimen did not crack the paint, showing no sign of poor adhesion. However, in combination with the scratch, it is possible to see whether the paints adhere properly along the scratch.

These results are essential because, for example, in the tensile test, it is vital to accurately measure the history of deformation even when cracking, which can only be achieved with a properly adherent basecoat. In the test, P5 and P8 were excluded as they separated from the surface of all five of the seven remaining cleaners. The Erichsen tests had a dual role in the research, serving both a validation and a qualification function. In the first phase of the Erichsen tests, visual inspection was used to verify that the paints P3, P4, and P9 passed on all materials after pre-treatment with the remaining (SC0, SC1, SC2, SC4, SC5, SC8, SC9) cleaning agents.

From the ARAMIS evaluations of the Erichsen tests, the thickness reductions at the top of the specimens were collected and compared with the results of the gauge thickness measurements. Interesting conclusions can be drawn from the results. With the typically matte finish materials (A11, A13, A14, A15), the remaining paint/finish combinations performed well with defects below 10%. However, the A12 sample showed defects above 15%, with some specimens showing defects above 20–25%. The surface of the A12 sample is much shinier and has an outstanding surface quality compared to the other materials.

For surface qualities with an Ra of 0.005–0.05, the adhesion of the tested paints no longer gives a stable result for a DIC test, so it may be worthwhile to roughen the surface. This conclusion is supported by the durability tests' results, where A12 samples also performed worse. A further result of the durability test is that the P3 and the P9 paints can still be applied one week after surface was prepared, and in fact, the P3 paint can still be applied at two weeks. This experience may be helpful for longer-term DIC tests.

4. Conclusions

First of all, the authors must note that the manufacturers do not give an exact, usable chemical compositions for the cleaning agents or the paints; they only list the ingredients. Therefore, providing results and conclusions that can be supported scientifically and stand

up to interpretation is not easy. It was the reason why the authors did not address this in the recording and formulation of the conclusions.

Secondly, the authors have more than 10 years' experience in recording DIC measurements, enabling us to guarantee adequate and appropriate preparation, and ensuring identical speckle patterns for all specimens.

The experiments and their results presented in this paper have demonstrated that different surface cleaning agents and spray formulations of white/clear paints behave differently on aluminum sheet materials. It has been demonstrated that the present part of cleaning agents or paints cannot be used in the preparatory operations of DIC tests. It has been shown that paints that appear to be good by visual inspection do not adhere properly to the material and separate from the surface when deformed, so the transmission of deformations is not achieved, giving incorrect results. It was found that the P3, P4, and P9 paints performed well on all samples in conjunction with the cleaning agents SC0, SC1, SC2, SC4, SC5, SC8, and SC9. Considering also the results of the long-term endurance tests, P3 performed the best, which is significant for tests of long duration or even several weeks.

With regard to future research opportunities, the authors suggest and anticipate obtaining larger quantities of aluminum sheets, cleaners, and spray paints from the same batch and storing them in different but strictly controlled environments so that they are exposed to different temperatures, humidity, UV radiation, etc.; this creates the opportunity to analyze to what extent and how these environmental factors affect the behavior of the paints when they are applied to the sheets. Such a study could combine the series of tests described previously here with the Erichsen cupping test and DIC measurements. Furthermore, it could be exciting to expose pre-painted plates to different effects. However, these would require a significant number of combinations and would also present a major challenge to researchers in terms of cost and measurement time.

Author Contributions: Conceptualization, S.S. and V.F.; methodology, S.S.; software, S.S. and V.F.; validation, S.S. and V.F.; formal analysis, S.S. and V.F.; investigation, S.S., V.F., D.K., A.N., M.S. and S.F.; resources, S.S., A.N. and S.F.; data curation, S.S. and V.F.; writing—original draft preparation, S.S., V.F., D.K., A.N., M.S. and S.F.; writing—review and editing, S.S., V.F., D.K., A.N., M.S. and S.F.; visualization, S.S. and V.F.; supervision, D.K., A.N., M.S. and S.F.; project administration, S.S.; funding acquisition, S.F. All authors have read and agreed to the published version of the manuscript.

Funding: This research received no external funding.

Data Availability Statement: Not applicable.

Acknowledgments: This paper was prepared by the research team "SZE-RAIL".

Conflicts of Interest: The authors declare no conflict of interest.

Abbreviations

2D	two dimension(s)/two dimensional
2D-DIC	two dimensional digital image correlation
3D	three dimension(s)/three dimensional
3D-DIC	three dimensional digital image correlation
3DMC-DIC	three-dimensional subset-based digital image correlation
CCD	charged-coupled device
DIC	digital image correlation
ESPI	electronic speckle pattern interferometry
FE	finite element
FEM	finite element method or finite element model
FSW	friction stir weldings
ISO	International Organization for Standardization
RSDIC	reflection-assisted stereo digital image correlation
SB-DIC	stress-block coupled digital image correlation
SDIC	stereo digital image correlation

References

1. Dong, Y.L.; Pan, B. A Review of Speckle Pattern Fabrication and Assessment for Digital Image Correlation. *Exp. Mech.* **2017**, *57*, 1161–1181. [[CrossRef](#)]
2. Gencturk, B.; Hossain, K.; Kapadia, A.; Labib, E.; Mo, Y.L. Use of Digital Image Correlation Technique in Full-Scale Testing of Prestressed Concrete Structures. *Measurement* **2014**, *47*, 505–515. [[CrossRef](#)]
3. Yates, J.R.; Zanganeh, M.; Tai, Y.H. Quantifying Crack Tip Displacement Fields with DIC. *Eng. Fract. Mech.* **2010**, *77*, 2063–2076. [[CrossRef](#)]
4. Reu, P.L.; Rohe, D.P.; Jacobs, L.D. Comparison of DIC and LDV for Practical Vibration and Modal Measurements. *Mech. Syst. Signal Process.* **2017**, *86*, 2–16. [[CrossRef](#)]
5. Sebastiani, M.; Eberl, C.; Bemporad, E.; Pharr, G.M. Depth-Resolved Residual Stress Analysis of Thin Coatings by a New FIB-DIC Method. *Mater. Sci. Eng. A* **2011**, *528*, 7901–7908. [[CrossRef](#)]
6. Gao, G.; Huang, S.; Xia, K.; Li, Z. Application of Digital Image Correlation (DIC) in Dynamic Notched Semi-Circular Bend (NSCB) Tests. *Exp. Mech.* **2015**, *55*, 95–104. [[CrossRef](#)]
7. Lava, P.; Cooreman, S.; Coppieeters, S.; de Strycker, M.; Debryne, D. Assessment of Measuring Errors in DIC Using Deformation Fields Generated by Plastic FEA. *Opt. Lasers Eng.* **2009**, *47*, 747–753. [[CrossRef](#)]
8. Kapor, M.; Skejić, A.; Medić, S.; Balić, A. DIC Assessment of Foundation Soil Response for Different Reinforcement between Base and Soft Subgrade Layer—Physical Modeling. *Geotext. Geomembr.* **2023**. [[CrossRef](#)]
9. Chen, Y.; Yang, J.; Qiu, X.; Ji, C.; Wang, B. DIC-Based Constant Amplitude and Two-Block Loading Fatigue Life Prediction of Open Hole GLARE Laminate. *Eng. Fract. Mech.* **2023**, *278*, 109016. [[CrossRef](#)]
10. Ma, K.; Liu, Z.; Wang, B.; Zhang, H.; Song, Q.; Liu, H. In-Situ DIC Measurement of Material Deformation through Spatial-Temporal Kinematics Analysis during Orthogonal Cutting Ti6Al4V. *Measurement* **2023**, *207*, 112367. [[CrossRef](#)]
11. Wang, L.; Liu, G.; Deng, Y.; Sun, W.; Ma, Q.; Ma, S. Investigation on Out-of-Plane Displacement Measurements of Thin Films via a Mechanical Constraint-Based 3D-DIC Technique. *Opt. Commun.* **2022**, *530*, 129015. [[CrossRef](#)]
12. Luo, H.; Yu, L.; Pan, B. Bi-Prism-Based Single-Bilateral-Telecentric-Camera Stereo-DIC for Accurate Underwater 3D Deformation Measurement: Implementation of a Parametric Model. *Opt. Lasers Eng.* **2023**, *162*, 107440. [[CrossRef](#)]
13. Ye, M.; Liang, J.; Li, L.; Zong, Y.; Guo, J.; Tang, Z.; Ma, S.; Chen, R. Simultaneous Measurement of External and Internal Surface Shape and Deformation Based on Photogrammetry and Stereo-DIC. *Opt. Lasers Eng.* **2022**, *158*, 107179. [[CrossRef](#)]
14. Pupurs, A.; Loukil, M.; Varna, J. Digital Image Correlation (DIC) Validation of Engineering Approaches for Bending Stiffness Determination of Damaged Laminates. *Appl. Compos. Mater.* **2022**, *29*, 1937–1958. [[CrossRef](#)]
15. Suthar, H.; Bhattacharya, A.; Paul, S.K. DIC-Based Approach to Predict Post Necking Behavior for AA6061, AA7075 and Their Friction Stir Welded Joints. *Mech. Mater.* **2022**, *172*, 104364. [[CrossRef](#)]
16. Bhuiyan, A.; Willis, J.M.; Dugnani, R.; Trujillo-Wheeler, F. Digital Image Correlation (DIC) Techniques in Learning Classical Mechanics. In Proceedings of the ASEE Annual Conference and Exposition, Conference Proceedings, Minneapolis, MN, USA, 25–29 June 2022.
17. Zhou, T.; Chen, J.; Xie, H.; Zhou, C.; Wang, F.; Zhu, J. Failure and Mechanical Behaviors of Sandstone Containing a Pre-Existing Flaw Under Compressive–Shear Loads: Insight from a Digital Image Correlation (DIC) Analysis. *Rock Mech. Rock Eng.* **2022**, *55*, 4237–4256. [[CrossRef](#)]
18. Li, S.; Lin, H.; Hu, S.; Cao, R.; Luo, X. Mechanical Behavior of Anchored Rock with an Infilled Joint under Uniaxial Loading Revealed by AE and DIC Monitoring. *Theor. Appl. Fract. Mech.* **2023**, *123*. [[CrossRef](#)]
19. Ramos, T.; Furtado, A.; Eslami, S.; Alves, S.; Rodrigues, H.; Arêde, A.; Tavares, P.J.; Moreira, P.M.G.P. 2D and 3D Digital Image Correlation in Civil Engineering—Measurements in a Masonry Wall. *Procedia Eng.* **2015**, *114*, 215–222. [[CrossRef](#)]
20. Tharun Kumar Reddy, K.; Koniki, S. Digital Image Correlation for Structural Health Monitoring—A Review. *E3S Web Conf.* **2021**, *309*, 01176. [[CrossRef](#)]
21. Kuchak, A.; Marinkovic, D.; Zehn, M. Parametric Investigation of a Rail Damper Design Based on a Lab-Scaled Model. *J. Vib. Eng. Technol.* **2021**, *9*, 51–60. [[CrossRef](#)]
22. Kuchak, A.; Marinkovic, D.; Zehn, M. Finite Element Model Updating—Case Study of a Rail Damper. *Struct. Eng. Mech.* **2020**, *73*, 27–35. [[CrossRef](#)]
23. Macura, D.; Laketić, M.; Pamučar, D.; Marinković, D. Risk Analysis Model with Interval Type-2 Fuzzy FMEA—Case Study of Railway Infrastructure Projects in the Republic of Serbia. *Acta Polytech. Hung.* **2022**, *19*, 103–118. [[CrossRef](#)]
24. Fischer, S.; Kocsis Szürke, S. Detection Process of Energy Loss in Electric Railway Vehicles. *Facta Univ. Ser. Mech. Eng.* **2023**, 11368. [[CrossRef](#)]
25. Kurhan, D.; Fischer, S. Modeling of the Dynamic Rail Deflection Using Elastic Wave Propagation. *J. Appl. Comput. Mech.* **2022**, *8*, 379–387. [[CrossRef](#)]
26. Gáspár, L.; Bencze, Z. Increasing Life Expectancy of Road Pavements. *Gradjevinar* **2020**, *72*, 515–522. [[CrossRef](#)]
27. He, L.; Cai, H.; Huang, Y.; Ma, Y.; van den Bergh, W.; Gaspar, L.; Valentin, J.; Vasiliev, Y.E.; Kowalski, K.J.; Zhang, J. Research on the Properties of Rubber Concrete Containing Surface-Modified Rubber Powders. *J. Build. Eng.* **2021**, *35*, 101991. [[CrossRef](#)]
28. Tóth, C.; Primusz, P. Development of a Road Pavement Structure Diagnostic. *Coatings* **2022**, *12*, 1944. [[CrossRef](#)]
29. Király, T.; Primusz, P.; Tóth, C. Simulation of Static Tyre–Pavement Interaction Using Two FE Models of Different Complexity. *Appl. Sci.* **2022**, *12*, 2388. [[CrossRef](#)]

30. Lipski, A. Change of Specimen Temperature during the Monotonic Tensile Test and Correlation between the Yield Strength and Thermoelasto-Plastic Limit Stress on the Example of Aluminum Alloys. *Materials* **2021**, *14*, 13. [\[CrossRef\]](#)
31. Gao, H.; Sheikholeslami, G.; Dearden, G.; Edwardson, S.P. Reverse Analysis of Scan Strategies for Controlled 3D Laser Forming of Sheet Metal. *Procedia Eng.* **2017**, *183*, 369–374. [\[CrossRef\]](#)
32. Sych, O.V.; Korotovskaya, S.V.; Khlusova, E.I.; Motovilina, G.D.; Nikitina, V.R.; Sych, O.V.; Korotovskaya, S.V.; Khlusova, E.I.; Motovilina, G.D.; Nikitina, V.R. Heterogeneity of Structure and Mechanical Properties Studied in Thickness up to 100 Mm of Low-Alloy Shipbuilding Steel Sheets with a Yield Strength Not Less Th. *Inorg. Mater. Appl. Res.* **2022**, *13*, 1477–1489. [\[CrossRef\]](#)
33. Ajay, C.V.; Elangovan, S.; Pratheesh Kumar, S.; Manisekar, K. Multi-Objective Optimization in Incremental Sheet Forming of Ti-6Al-4V Alloy Using Grey Relational Analysis Method. *Proc. Inst. Mech. Eng. Part E J. Process Mech. Eng.* **2022**, *236*, 1467–1476. [\[CrossRef\]](#)
34. Shunmugesh, K.; Raphel, A.; Unnikrishnan, T.G.; Akhil, K.T. Finite Element Modelling of Carbon Fiber Reinforced with Vespel and Honey-Comb Structure. *Mater. Today Proc.* **2022**, *72*, 2163–2168. [\[CrossRef\]](#)
35. Reu, P. Speckles and Their Relationship to the Digital Camera. *Exp. Tech.* **2014**, *38*, 1–2. [\[CrossRef\]](#)
36. Reu, P. All about Speckles: Speckle Density. *Exp. Tech.* **2015**, *39*, 1–2. [\[CrossRef\]](#)
37. Lionello, G.; Cristofolini, L. A Practical Approach to Optimizing the Preparation of Speckle Patterns for Digital-Image Correlation. *Meas. Sci. Technol.* **2014**, *25*, 107001. [\[CrossRef\]](#)
38. Reu, P.L. A Realistic Error Budget for Two Dimension Digital Image Correlation. *Conf. Proc. Soc. Exp. Mech. Ser.* **2016**, *3*, 181–187. [\[CrossRef\]](#)
39. Reu, P. Points on Paint. *Exp. Tech.* **2015**, *39*, 1–2. [\[CrossRef\]](#)
40. Szalai, S.; Dogossy, G. Speckle Pattern Optimization for DIC Technologies. *Acta Tech. Jaurinensis* **2021**, *14*, 228–243. [\[CrossRef\]](#)
41. Nasri, M.T.; Abbassi, F.; Ahmad, F.; Makhoulfi, W.; Ayadi, M.; Mehboob, H.; Choi, H.S. Experimental and Numerical Investigation of Sheet Metal Failure Based on Johnson-Cook Model and Erichsen Test over a Wide Range of Temperatures. *Mech. Adv. Mater. Struct.* **2022**. [\[CrossRef\]](#)
42. Komori, K.; Matsushima, K. Predicting Ductile Fracture during Biaxial Sheet Stretching Using an Ellipsoidal Void Model. *Theor. Appl. Fract. Mech.* **2022**, *118*, 103215. [\[CrossRef\]](#)
43. Rubešová, K.; Rund, M.; Rzepa, S.; Jirková, H.; Jeníček, Š.; Urbánek, M.; Kučerová, L.; Konopík, P. Determining Forming Limit Diagrams Using Sub-Sized Specimen Geometry and Comparing FLD Evaluation Methods. *Metals* **2021**, *11*, 484. [\[CrossRef\]](#)
44. Sangkharat, T.; Dechjarern, S. Using Image Processing on Erichsen Cup Test Machine to Calculate Anisotropic Property of Sheet Metal. *Procedia Manuf.* **2019**, *29*, 390–397. [\[CrossRef\]](#)
45. Zhang, L.; Min, J.; Carsley, J.E.; Stoughton, T.B.; Lin, J. Experimental and Theoretical Investigation on the Role of Friction in Nakazima Testing. *Int. J. Mech. Sci.* **2017**, *133*, 217–226. [\[CrossRef\]](#)
46. Wang, Y.; Lava, P.; Coppieters, S.; Houtte, P.V.; Debruyne, D. Application of a Multi-Camera Stereo DIC Set-up to Assess Strain Fields in an Erichsen Test: Methodology and Validation. *Strain* **2013**, *49*, 190–198. [\[CrossRef\]](#)
47. Sutton, M.A.; Orteu, J.J.; Schreier, H.W.; Reu, P. Introduction to Digital Image Correlation: Best Practices and Applications. *Exp. Tech.* **2012**, *36*, 3–4. [\[CrossRef\]](#)
48. Sorce, F.S.; Ngo, S.; Lowe, C.; Taylor, A.C. Quantification of Coating Surface Strains in Erichsen Cupping Tests. *J. Mater. Sci.* **2019**, *54*, 7997–8009. [\[CrossRef\]](#)
49. Szalai, S.; Szívós, B.F.; Kurhan, D.; Németh, A.; Sysyn, M.; Fischer, S. Optimization of Surface Preparation and Painting Processes for Railway and Automotive Steel Sheets. *Infrastructures* **2023**, *8*, 28. [\[CrossRef\]](#)
50. ISO 2808:2019; Paints and Varnishes—Determination of Film Thickness. International Organization for Standardization: Geneva, Switzerland, 2019; p. 49.
51. ISO 9117-6:2012; Paints and Varnishes—Drying Tests—Part 6: Print-Free Test. International Organization for Standardization: Geneva, Switzerland, 2012; p. 4.
52. ISO 9117-5:2012; Paints and Varnishes—Drying Tests—Part 5: Modified Bandow-Wolff Test. International Organization for Standardization: Geneva, Switzerland, 2012; p. 5.
53. ISO 2409:2020; Paints and Varnishes—Cross-Cut Test. International Organization for Standardization: Geneva, Switzerland, 2010; p. 14.
54. ISO 1519:2011; Paints and Varnishes—Bend Test (Cylindrical Mandrel). International Organization for Standardization: Geneva, Switzerland, 2011; p. 9.
55. ISO 1518-1:2019; Paints and Varnishes—Determination of Scratch Resistance—Part 1: Constant-Loading Method. International Organization for Standardization: Geneva, Switzerland, 2019; p. 8.
56. ISO 20482:2013; Metallic Materials—Sheet and Strip—Erichsen Cupping Test. International Organization for Standardization: Geneva, Switzerland, 2013; p. 7.
57. ISO 2768-1; General Tolerances—Part 1: Tolerances for Linear and Angular Dimensions without Individual Tolerance Indications. International Organization for Standardization: Geneva, Switzerland, 1989; p. 3.

Disclaimer/Publisher’s Note: The statements, opinions and data contained in all publications are solely those of the individual author(s) and contributor(s) and not of MDPI and/or the editor(s). MDPI and/or the editor(s) disclaim responsibility for any injury to people or property resulting from any ideas, methods, instructions or products referred to in the content.